The Plant Cell, Vol. 22: 62–76, January 2010, www.plantcell.org

BLADE-ON-PETIOLE1 Coordinates Organ Determinacy and Axial Polarity in *Arabidopsis* by Directly Activating ASYMMETRIC LEAVES2 [C][W]

Ji Hyung Jun,[a,b,1] Chan Man Ha,[a,b,1] and Jennifer C. Fletcher[a,b,2]

[a] Plant Gene Expression Center, U.S. Department of Agriculture/University of California at Berkeley, Albany, California 94710
[b] Department of Plant and Microbial Biology, University of California at Berkeley, Berkeley, California 94720

Continuous organ formation is a hallmark of plant development that requires organ-specific gene activity to establish determinacy and axial patterning, yet the molecular mechanisms that coordinate these events remain poorly understood. Here, we show that the organ-specific BTB-POZ domain proteins BLADE-ON-PETIOLE1 (BOP1) and BOP2 function as transcriptional activators during *Arabidopsis thaliana* leaf formation. We identify as a direct target of BOP1 induction the *ASYMMETRIC LEAVES2* (*AS2*) gene, which promotes leaf cell fate specification and adaxial polarity. We find that BOP1 associates with the *AS2* promoter and that BOP1 and BOP2 are required for *AS2* activation specifically in the proximal, adaxial region of the leaf, demonstrating a role for the BOP proteins as proximal-distal as well as adaxial-abaxial patterning determinants. Furthermore, repression of *BOP1* and *BOP2* expression by the indeterminacy-promoting *KNOX* gene *SHOOTMERISTEMLESS* is critical to establish a functional embryonic shoot apical meristem. Our data indicate that direct activation of *AS2* transcription by BOP1 and BOP2 is vital for generating the conditions for *KNOX* repression at the leaf base and may represent a conserved mechanism for coordinating leaf morphogenesis with patterning along the adaxial-abaxial and the proximal-distal axes.

INTRODUCTION

Higher plant development is a continuous process of organogenesis sustained by pluripotent stem cell reservoirs at the growing tips, the apical meristems. Establishment and maintenance of the shoot apical meristem (SAM) depends on the activity of class I *KNOTTED1*-like homeobox (*KNOX*) genes that are highly expressed in meristem cells (Lincoln et al., 1994; Dockx et al., 1995; Long et al., 1996; Belles-Boix et al., 2006). Lateral organs such as leaves initiate as small groups of homogeneous founder cells on the flanks of the SAM, and during early morphogenesis, these primordia become patterned along three axes of polarity: the adaxial-abaxial, proximal-distal, and medial-lateral axes. Subsequent growth and differentiation result in the elaboration of a mature three-dimensional leaf structure with a proximal petiole and a distal blade in simple-leaved species such as *Arabidopsis thaliana*. In contrast with adaxial-abaxial polarity, about which much is known, the molecular mechanisms that specify proximal-distal polarity in plants are very poorly understood.

The author responsible for distribution of materials integral to the findings presented in this article in accordance with the policy described in the Instructions for Authors (www.plantcell.org) is: Jennifer C. Fletcher (jfletcher@berkeley.edu).
[C]Some figures in this article are displayed in color online but in black and white in the print edition.
[W]Online version contains Web-only data.
[1] These authors contributed equally to this work.
[2] Address correspondence to jfletcher@berkeley.edu.
www.plantcell.org/cgi/doi/10.1105/tpc.109.070763

Lateral organ morphogenesis and patterning processes require extensive genome reprogramming. Initiation of a determinant leaf structure is closely associated with repression of *KNOX* gene expression in the organ founder cells (Jackson et al., 1994; Long et al., 1996). In *Arabidopsis*, the Myb gene *ASYMMETRIC LEAVES1* (*AS1*) is expressed in lateral organ primordia in a reciprocal pattern to that of the class I *KNOX* gene *SHOOTMERISTEMLESS* (*STM*), and *STM* represses *AS1* expression in the SAM (Byrne et al., 2000). AS1 and the LOB domain protein AS2 in turn stably silence the class I *KNOX* genes *BP* and *KNAT2* in developing leaf primordia (Byrne et al., 2000, 2002; Ori et al., 2000; Semiarti et al., 2001; Guo et al., 2008) by forming a complex with the chromatin-remodeling factor HIRA (Phelps-Durr et al., 2005). In addition, *AS1*, which is expressed throughout young leaf primordia, and *AS2*, which is specifically expressed in the adaxial domain of lateral organs, promote adaxial leaf identity and gene expression (Lin et al., 2003; Xu et al., 2003; Li et al., 2005; Ueno et al., 2007). Yet despite the critical roles *AS1* and *AS2* play in lateral organ morphogenesis, little is known about the upstream factors that induce their specific expression in organ primordia.

The *BLADE-ON-PETIOLE1* (*BOP1*) and *BOP2* genes play important roles in regulating leaf morphogenesis and patterning (Ha et al., 2003, 2007). *bop1-1* dominant-negative and *bop1 bop2* null mutants form ectopic outgrowths of blade tissue along the petioles of cotyledons and leaves, suggesting a role in proximal-distal pattern formation, and the *BOP* genes negatively regulate expression of the class I *KNOX* genes *BP*, *KNAT2*, and *KNAT6* in developing leaf primordia (Ha et al., 2003, 2007). BOP1 and BOP2 upregulate the expression of three members of the

AS2/LOB family (Iwakawa et al., 2002; Shuai et al., 2002; Matsumura et al., 2009), *AS2*, *ASL4/LOB*, and *ASL1/LBD36*, in leaf primordia (Ha et al., 2007). They also promote adaxial organ identity, positively regulating the expression of the adaxial polarity genes *PHB* and *PHV* as well as negatively regulating the expression of the abaxial polarity genes *FIL* and *KAN1* (Ha et al., 2007). BOP1 and BOP2 belong to a family of BTB/POZ domain and ankyrin repeat-containing proteins that includes the plant defense response regulator NPR1 and are expressed in a small group of proximal, adaxial lateral organ cells adjacent to the meristem-organ boundary (Ha et al., 2004; Hepworth et al., 2005). Although NPR1 is known to be a transcriptional regulator that mediates salicylic acid (SA)–induced gene expression in association with TGA family transcription factors (Cao et al., 1997; Zhang et al., 1999; Despres et al., 2000, 2003), the regulatory mechanism through which BOP1 and BOP2 influence organ morphogenesis is unknown.

In this study, we show that BOP1 and BOP2 regulate key organogenic events in the proximal region of *Arabidopsis* cotyledon and leaf primordia. We find that BOP1 and BOP2 proteins can dimerize in vivo and function as transcriptional coactivators when recruited to target gene promoters. We demonstrate that BOP1/2 activity is required for *AS2* activation specifically in the proximal region of the leaf and that BOP1 is a direct upstream regulator of *AS2* during leaf development that binds to sites in the *AS2* promoter containing a bZIP binding motif. Furthermore, we show that *STM* represses *BOP1* and *BOP2* expression in the embryonic SAM and that the absence of BOP activity permits ectopic shoot meristem formation in *stm* seedlings. Our data suggest that *BOP1* and *BOP2* regulate leaf morphogenesis along the proximal-distal axis by directly inducing *AS2* transcription at the leaf base, establishing the conditions for repression of class I *KNOX* gene expression to correctly pattern the petiole tissues.

RESULTS

BOP1 and BOP2 Function as Transcriptional Activators

To better understand the molecular mechanism of BOP1 and BOP2 activity, we took NPR1 as a paradigm for the family. NPR1 has a dual nuclear and cytoplasmic subcellular localization pattern (Despres et al., 2000), and nuclear-localized NPR1 provides transcriptional activation activity for defense gene induction (Rochon et al., 2006). A dual subcellular localization pattern has also been observed for BOP2 (Hepworth et al., 2005), and we likewise detected BOP1-green fluorescent protein fusions in both the nucleus and the cytoplasm (see Supplemental Figure 1 online). Based on these data, we hypothesized that BOP1 and BOP2, like NPR1, might function as transcriptional activators.

We tested whether the BOP proteins could stimulate transcription when tethered to DNA by assaying constructs consisting of the Gal4 DNA binding domain (BD) fused to either BOP1 (BD-BOP1) or BD-BOP2 (Figure 1A) in in vivo plant transcription assays (Huq et al., 2004). Transfection of unfused BOP1 or BOP2 did not generate luciferase activation beyond the baseline level of transcription (Figure 1B). By contrast, transfection with BD-BOP1 or BD-BOP2 activated transcription 11.2- and 8.6-fold above the baseline level, respectively (Figure 1B). Cotransfection of BD-BOP1 with BD-BOP2 produced similar fold induction values to those of BD-BOP1 or BD-BOP2 alone (Figure 1B). These results demonstrate that BOP1 and BOP2 have the capacity to activate transcription, dependent on their recruitment to the target promoter.

Because *bop1-1* plants exhibited dominant-negative phenotypes similar to those of *bop1-4 bop2-11* plants (Ha et al., 2004), we assessed whether mutant bop1-1 protein could inhibit wild-type BOP transactivation activity. bop1-1 protein fused to the Gal4 BD (BD-b1-1) showed no transactivation activity (Figure 1B), indicating that the addition of four amino acids to the C terminus of the BOP1 protein completely abolished its transcriptional activation capacity. In the presence of bop1-1 protein, the transactivation capacity of wild-type BOP1 and BOP2 protein was strongly reduced (Figure 1B). Thus, bop1-1 protein either interferes with the transactivation function of the wild-type BOP proteins or itself functions as a transcriptional inhibitor.

Next, we tested for potential interactions between the BOP1, BOP2, and bop1-1 proteins. In the yeast two-hybrid system, BOP1 and BOP2 protein fused to the Gal4 DNA BD showed autoactivation activity when tested with the control empty vector (E) containing the activation domain (AD). Nonetheless, we could clearly detect pairwise interactions between the BOP1, BOP2, and bop1-1 proteins (Figure 1C). The BOP1 and BOP2 proteins showed equally strong interactions as homodimers and heterodimers (Figure 1C). Using bimolecular fluorescence complementation assays, we verified that both BOP1 and BOP2 form homodimers in planta and that BOP1 and BOP2 can also heterodimerize (Figure 1D). These interactions were observed in both the cytoplasm and the nucleus. bop1-1 protein interacted strongly in the nucleus and more weakly in the cytosol with both BOP1 and BOP2 proteins (Figure 1D). We conclude that BOP1 and BOP2 can physically interact to form homodimers and heterodimers and that bop1-1 mutant protein can interact with both wild-type proteins, potentially to attenuate their abilities to activate target gene transcription.

Nuclear Localization of BOP1 Protein Is Necessary and Sufficient for Biological Function

To determine the biological relevance of BOP1 protein localization in the nucleus, we generated a translational fusion of BOP1 to the hormone binding domain of the rat glucocorticoid receptor (BOP1-GR) and transformed this construct into Landsberg *erecta* (L*er*), *bop1-1*, and *bop1-4 bop2-11* plants. Application of dexamethasone (Dex) hormone leads to translocation of the GR fusion protein from the cytoplasm to the nucleus (see Supplemental Figure 2 online). After a 4-h Dex treatment, BOP1-GR fusion protein was enriched in the nuclear fraction compared with non-Dex-treated fractions (see Supplemental Figure 2 online). These results show that BOP1:GR fusion protein is translocated into the nucleus in a steroid-dependent manner.

The development of $35S_{pro}$*:BOP1-GR* L*er* plants was indistinguishable from that of wild-type L*er* plants in the absence of hormone (Figures 2A and 2B). Following Dex treatment, $35S_{pro}$*:BOP1-GR* L*er* plants displayed upward curling leaf phenotypes (Figures 2C and 2D) characteristic of *BOP1* gain-of-function

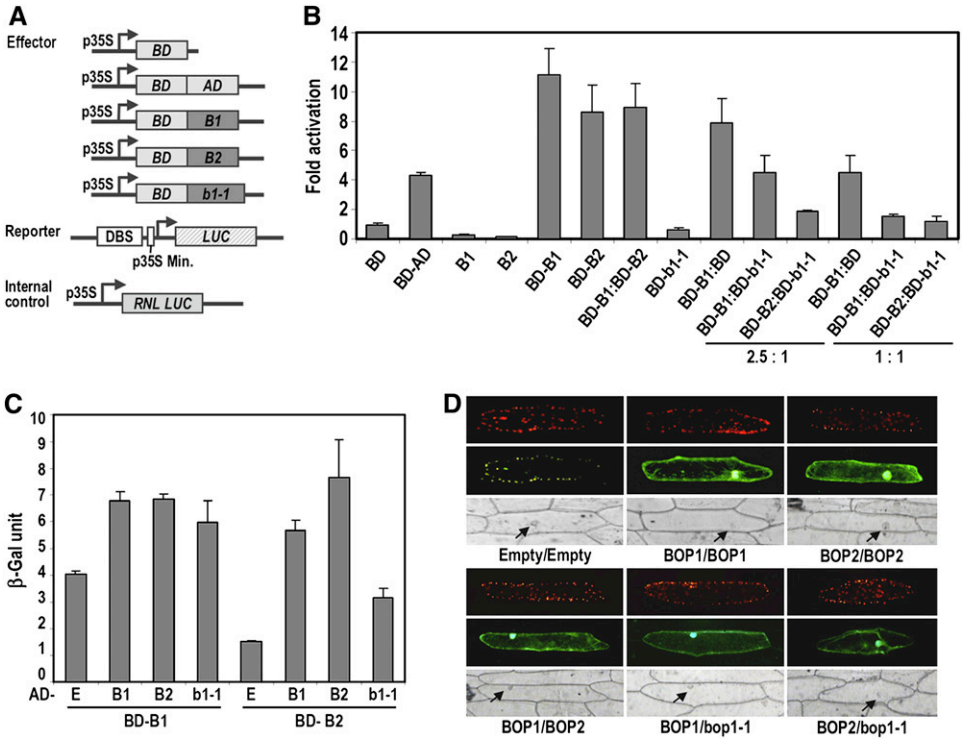

Figure 1. Functional Analysis of the BOP Proteins.

(A) Schematics of the constructs used for the transactivation assays: AD:GAL4 activation domain, BD:GAL4 DNA binding domain, DBS:GAL4 binding site, LUC:Firefly Luciferase, RNL LUC:Renilla Luciferase, B1:BOP1, and B2:BOP2.

(B) Transcription activation assays of BOP1, BOP2, and bop1-1 recruited to DNA through the Gal4 BD (BD-B1:BD-BOP1, BD-B2:BD-BOP2, and BD-b1-1:BD-bop1-1). Gal4 BD-AD and BD were used as positive and negative controls, respectively. Wild-type BD-BOP1 or BD-BOP2 construct was mixed with mutant BD-bop1-1 construct at a 2.5:1 ratio or a 1:1 ratio. RNL LUC was used as internal control to measure the photon count ratio of the reporter LUC and RNL LUC for each sample. B1 and B2 indicate BOP1 and BOP2 protein expressed alone. Fold activation represents the relative luciferase units obtained for the given construct(s) divided by those obtained with the unfused Gal4 BD construct alone (n = 9). Error bars represent SD.

(C) β-Galactosidase assays quantifying reporter gene expression in the yeast two-hybrid interactions. Error bars represent SD (n = 9). E, empty vector.

(D) In planta bimolecular fluorescence complementation assays. Combinations of constructs are shown below the images. A yellow fluorescent protein (YFP) signal (green, middle panel) indicates a physical interaction between proteins. A *35S$_{pro}$:RFP* construct (red, top panel) was used to determine transformation efficiency. Arrows point to the locations of the nuclei under bright field (bottom panel).

plants (Figure 2E). A subtle distinction between the two is that in *35S$_{pro}$:BOP1-GR* L*er* plants, this upward curling can occur toward the tip of the blade, causing waving of the leaves (Figure 2D), whereas *35S$_{pro}$:BOP1* L*er* leaves show upward curling more prevalently along the margins (Figure 2E). By contrast, untransformed wild-type L*er* plants grown in the presence of Dex showed no phenotypic changes (see Supplemental Figure 3 online). Thus, the upward curling leaf phenotypes observed in the *35S$_{pro}$:BOP1-GR* L*er* plants is due to Dex-dependent ectopic activity of the BOP1-GR fusion protein.

Similarly, the development of *35S$_{pro}$:BOP1-GR bop1-1* transformants was indistinguishable from that of untransformed *bop1-1* plants in the absence of hormone (Figures 2F and 2G). *bop1-1* plants showed no phenotypic alterations in the presence of Dex (see Supplemental Figure 3 online), whereas *35S$_{pro}$:BOP1-GR bop1-1* plants displayed partial to near-complete rescue of the rosette leaf phenotypes (Figures 2H and 2I). In the presence of 10 μm Dex, the leaves of *35S$_{pro}$:BOP1-GR bop1-1* plants were mostly wild-type in appearance or displayed a single ectopic outgrowth, and some also showed strongly upward curling leaf phenotypes (Figures 2H and 2I) characteristic of *35S$_{pro}$:BOP1 bop1-1* (Figure 2J) plants. Similar results were obtained with *35S$_{pro}$:BOP1-GR bop1-4 bop2-11* plants (see Supplemental Figure 4 online). These data show that BOP1-GR fusion protein is biologically active in a hormone dose-dependent manner and that nuclear localization of BOP1 protein is necessary and sufficient for its biological function.

Activation of AS2 and ASL4/LOB by BOP1 Induction

We hypothesized that if BOP1 functions as a transcriptional activator in vivo, then it might directly regulate some of its known downstream target genes (Ha et al., 2007). To identify direct targets of BOP1 regulation, we examined the effect of BOP1-GR activation on the expression of candidate *ASL/LBD*, class I *KNOX*, and adaxial-abaxial polarity genes (Figure 3A). We found

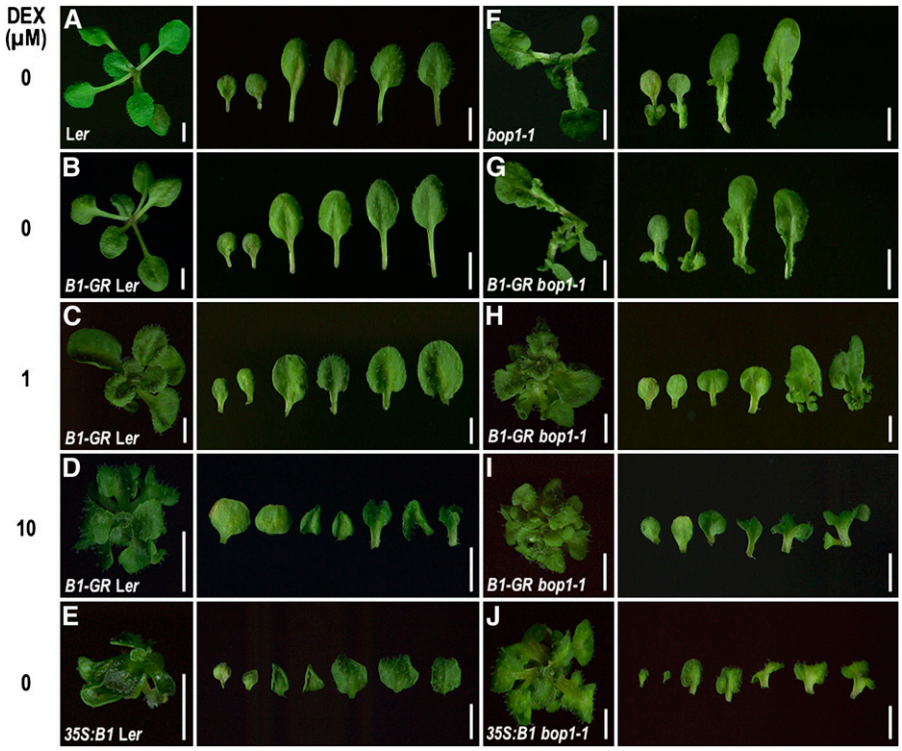

Figure 2. Dose Responsiveness of the *35S$_{pro}$:BOP1-GR* Phenotype.

(A) L*er*.
(B) to **(D)** *35S$_{pro}$:BOP1-GR* L*er*.
(E) *35S$_{pro}$:BOP1* L*er*.
(F) *bop1-1*.
(G) to **(I)** *35S$_{pro}$:BOP1-GR bop1-1*.
(J) *35S$_{pro}$:BOP1 bop1-1*.
Representative 16-d-old whole plants (left panel) and heteroblastic leaf series (right panel) from cotyledons up to leaf number two, four, or five are shown for each line after incubation in the indicated concentration of Dex. Bars = 10 mm in **(A)**, **(B)**, **(F)**, and **(G)** and 5 mm in **(C)** to **(E)** and **(H)** to **(J)**.

that *AS2* and *ASL4*/*LOB* mRNA levels were elevated within 4 and 24 h, respectively, of Dex treatment (Figure 3A). In a time course of Dex induction in *35S$_{pro}$:BOP1-GR bop1-1* and *bop1-1* plants, *AS2* expression was induced as early as 1 h after Dex application and continuously increased over the 24-h time course (Figure 3B). By contrast, increased *ASL4*/*LOB* expression only became detectable 4 to 8 h after induction. These data are consistent with *AS2* being an immediate target and *ASL4*/*LOB* being an indirect target of BOP1 activation.

Rapid activation of *AS2* transcription suggested that it might occur independently of protein synthesis. We tested this hypothesis by analyzing *AS2* expression in response to Dex induction in the presence of the protein synthesis inhibitor cycloheximide (CHX) (Figure 3C). The effect of CHX was monitored by examining the expression of *IAA1* (see Supplemental Figure 5 online), which is strongly induced by CHX alone (Abel et al., 1995). Combined Dex plus CHX treatment resulted in the induction of *AS2* mRNA similarly to Dex treatment alone (Figure 3C; see Supplemental Figure 5 online). Thus, the rapid induction of *AS2* by BOP1 does not require protein synthesis, indicating that *AS2* is likely a direct transcriptional target of BOP1.

We determined in which tissues BOP1 activates *AS2* expression by examining the activity of a promoter *AS2:GUS* reporter gene fusion in response to BOP1-GR induction. This *AS2$_{pro}$:GUS* construct, in which the GUS coding sequence was fused to 4776 bp of *AS2* upstream sequence, was sufficient to complement the *as2* phenotype. Consistent with previous reports (Iwakawa et al., 2007; Wu et al., 2008), the *AS2$_{pro}$:GUS* transgenic lines all showed the same pattern of GUS activity on the adaxial side of cotyledons and leaves, as well as in root tips (see Supplemental Figure 6 online). After 2 h of BOP1 induction, *AS2$_{pro}$:GUS* activity in *35S$_{pro}$:BOP1-GR bop1-1* plants was elevated in developing leaves and expanded more distally into the blade of mature leaves (Figure 3D). After 24 h of induction, ectopic GUS activity was observed throughout the blades of mature leaves and the base of the cotyledons. No change in *AS2$_{pro}$:GUS* activity was observed in *bop1-1* plants following 24 h of Dex treatment (Figure 3D). These data indicate that BOP1 is sufficient to activate *AS2* transcription in vegetative tissues and that the effect of BOP1 on the *AS2* promoter is likely to be direct.

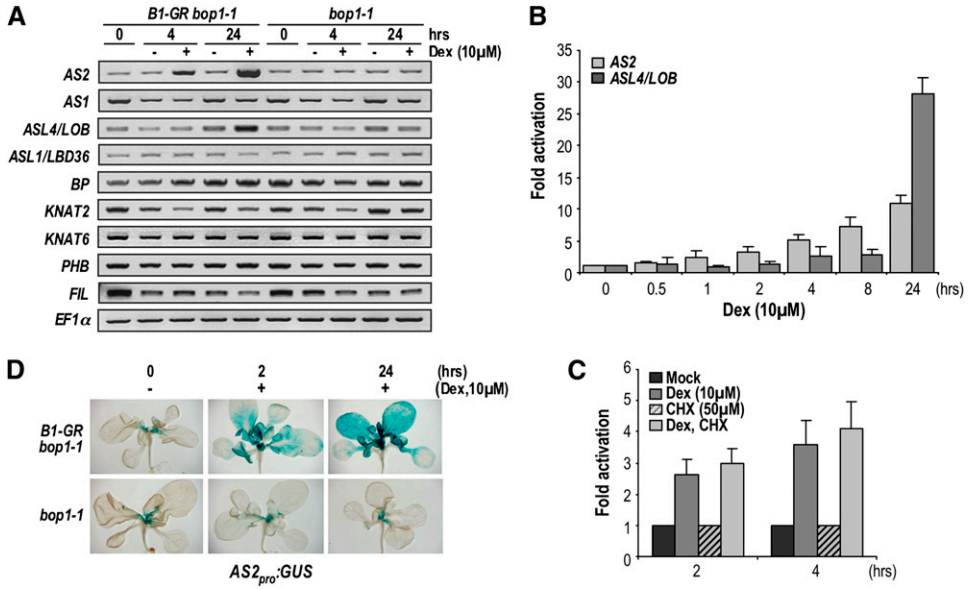

Figure 3. *AS2* Is an Immediate Target of BOP1.

(A) Expression profiles of *BOP1* downstream target genes. RT-PCR analysis of *AS1*, *AS2*, *ASL4/LOB*, *ASL1/LBD36*, *BP*, *KNAT2*, *KNAT6*, *PHB*, and *FIL* expression in 11-d-old *bop1-1* or *35S:BOP1-GR bop1-1* plants mock treated or treated with Dex for 0, 4, or 24 h. The PCR products were visualized using ethidium bromide staining, and *EF1α* was used as a control.
(B) Induction of *AS2* and *ASL4/LOB* expression in 11-d-old $35S_{pro}$*:BOP1-GR bop1-1* plants mock treated or treated with Dex for the indicated times.
(C) Relative temporal expression of *AS2* in 11-d-old $35S_{pro}$*:BOP1-GR bop1-1* plants after 2 or 4 h of mock, Dex, CHX, or Dex+CHX treatment. Expression values are normalized to the respective mock treatment control. Mean transcript levels in **(B)** and **(C)** were determined by real-time quantitative RT-PCR analyses of three biological replicates, normalized to *TUB4*. Error bars represent SD.
(D) $AS2_{pro}$*:GUS* activity in 11-d-old $35S_{pro}$*:BOP1-GR bop1-1* plants treated with 10 μM Dex for 0, 2, or 24 h.

BOP1 Directly Associates with the AS2 Promoter

To determine whether BOP1 directly associates with *AS2* regulatory sequences, we performed chromatin immunoprecipitation (ChIP) using BOP1-GR *bop1-1* transgenic plants. After determining that full-length BOP1-GR fusion protein in the nuclear fraction was specifically recognized by an anti-GR antibody (see Supplemental Figure 2 online), we performed ChIP assays using 11 sets of primers spanning 5 kb of the *AS2* upstream genomic sequence and coding region. Compared with the input and mock control, Dex-treated BOP1-GR *bop1-1* samples showed strong enrichment at sites IV, V, and VI in the promoter region (Figures 4A and 4B). Using quantitative PCR, we detected 25-fold enrichment of site V after Dex treatment (Figure 4A). ChIP assays performed on untransformed *bop1-1* plants showed no significant enrichment of the promoter regions tested, nor did the control *EF1α* and *TUB4* genomic regions. These data demonstrate that BOP1 associates in vivo with specific regulatory sites located in the *AS2* promoter and together with the transactivation results suggest that BOP1 functions in a transcriptional activator complex that acts directly at the *AS2* promoter.

AS2 Promoter Deletion Analysis

To confirm that the genomic region enriched in the ChIP assay was responsible for the specific regulation of *AS2* by BOP1 protein, we generated a series of β-glucuronidase (GUS) constructs containing deletions of the *AS2* 5′ regulatory region (Figure 4B). In the absence of Dex, BOP1-GR *bop1-1* plants carrying the pro-4.0 and pro-3.2 deletion constructs showed the same pattern of GUS activity (Figures $4D_1$ and $4E_1$) as plants carrying the pro-4.8 full-length promoter construct (Figure $4C_1$; see Supplemental Figure 6 online), indicating that the 3.2-kb upstream region contains all the *cis*-acting elements necessary for proper *AS2* expression. By contrast, plants carrying either the pro-2.6 or the pro-2.1 construct displayed very weak GUS activity, restricted to the adaxial domain of young leaf primordia and the early stage of ectopic outgrowth along the *bop1-1* petioles (Figures $4F_1$ and $4G_1$). Plants carrying the pro-1.0 construct displayed no GUS activity (Figure $4H_1$). The upstream region between 2.6 and 3.2 kb corresponds to sites IV, V, and VI with which BOP1 associates in the ChIP assays (Figures 4A and 4B), confirming the in vivo requirement for these BOP1 binding elements in the *AS2* promoter.

We next determined which regions of the *AS2* promoter responded to BOP1 induction by Dex treating BOP1-GR *bop1-1* plants carrying the various *AS2* promoter deletion constructs. After 24 h of Dex treatment, transgenic plants carrying the pro-4.8, pro-4.0, or pro-3.2 construct displayed ectopic GUS activity throughout the leaf blades, indicating a strong response to BOP1 activation (Figures $4C_2$ to $4E_2$). Lines carrying shorter constructs showed no Dex-dependent induction (Figures $4F_2$ to $4H_2$). These

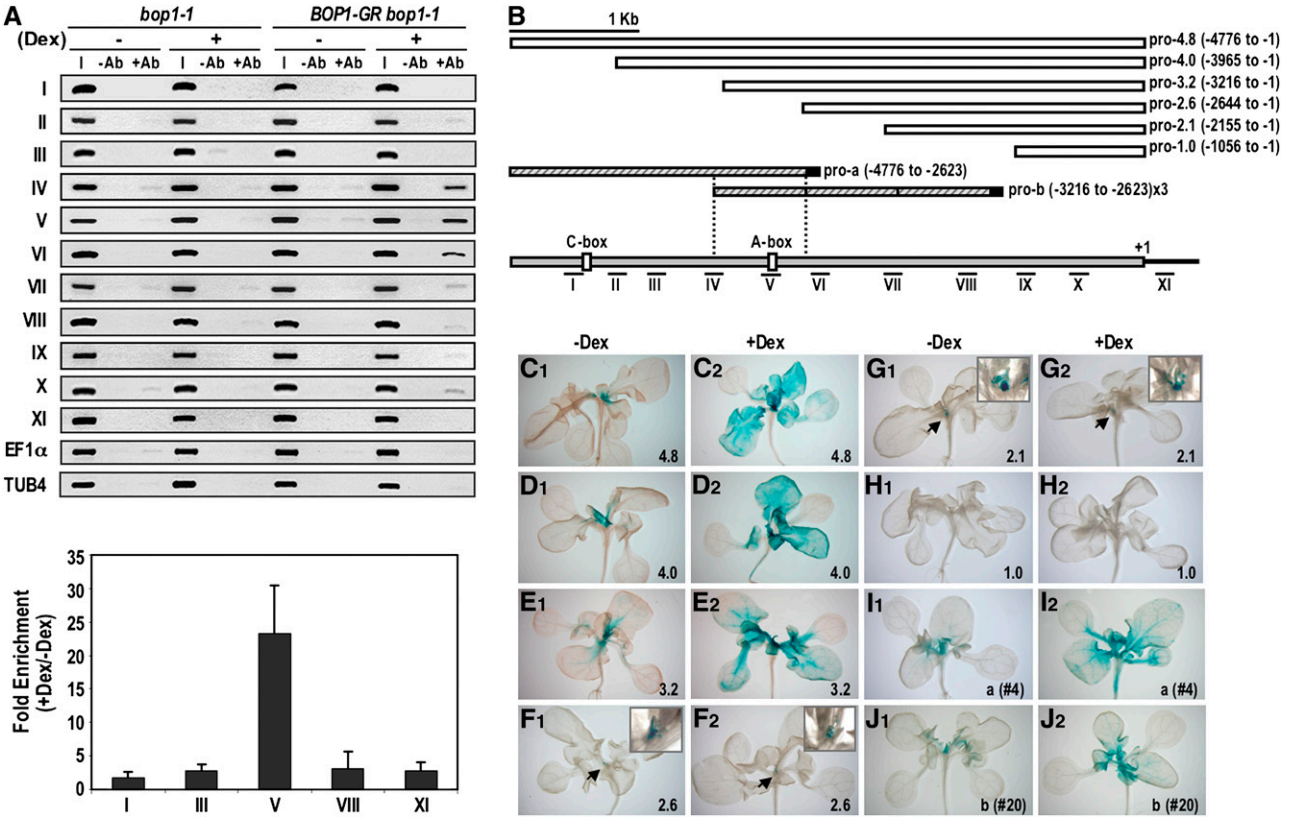

Figure 4. Identification of the Genomic Region Responsible for *AS2* Regulation by BOP1.

(A) Detection of *AS2* genomic fragments in *bop1-1* and *35S$_{pro}$:BOP1-GR bop1-1* seedlings after ChIP using anti-GR antiserum. Roman numerals denote 200- to 500-bp genomic fragments amplified from the *AS2* promoter and coding sequences (top). Enrichment of genomic fragments in *bop1-1* and *35S$_{pro}$:BOP1-GR bop1-1* samples after Dex treatment was quantified by real-time quantitative RT-PCR (bottom) after normalization to the unrelated *TUB4* control sequence. Error bars represent SD. I, input; −Ab, without antibody, +Ab, with antibody.

(B) Diagram of the *AS2* promoter (gray). White boxes indicate the 5′ regulatory fragments used in the GUS reporter constructs. Hatched boxes in pro-a and pro-b contain the region from −4776 to −2623 and a three tandem repeat of the region from −3216 to −2623, respectively, fused to a 35S minimal promoter (black boxes). The predicted A-box (−2818) and C-box (−4254) bZIP protein binding sites are indicated. The positions of the promoter regions analyzed by ChIP are shown at the bottom.

(C) to **(J)** Functional analysis of the *AS2* regulatory region. Representative expression patterns of *35S$_{pro}$:BOP1-GR bop1-1* plants carrying the *AS2$_{pro}$:GUS* reporter constructs diagramed in **(B)** are shown. Promoter activity was monitored after incubation in the presence (+) or absence (−) of 10 μM Dex for 24 h. Arrows indicate the SAM region, and magnified views of the shoot apices are shown in the boxes. The label in the lower right-hand corner indicates the *AS2* promoter deletion construct used.

data show that the region between 2.6 and 3.2 kb upstream of the *AS2* start site is required for the response of *AS2* to BOP1 activation.

We generated additional promoter constructs to confirm the importance of this BOP1-responsive region. The first contained the most distal region of the *AS2* promoter, from 2.6 to 4.8 kb (pro-a). The second contained three tandem repeats of the 2.6- to 3.2-kb region (pro-b). We analyzed *BOP1-GR bop1-1* lines with pro-a or pro-b driven GUS activity to determine their responsiveness to BOP1 activation. Thirteen lines carrying the pro-a construct showed weak GUS activity in young leaf primordia (Figure 4I$_1$). After Dex treatment, nine of these lines displayed expanded GUS staining into the proximal region of the maturing leaf blades (Figure 4I$_2$). Three lines carrying the pro-b construct showed weak GUS activity in young leaf primordia (Figure 4J$_1$), and after Dex treatment, all three showed expanded GUS activity into the proximal leaf blade (Figure 4J$_2$). These data demonstrate that the 2.6- to 3.2-kb region upstream of the *AS2* coding sequence is necessary and sufficient for *AS2* induction by BOP1 protein.

AS2 Activation by BOP1 and BOP2 in the Proximal Leaf Domain

To determine in which tissues BOP1 protein activates *AS2* expression in vivo, we examined the activity of a *AS2$_{pro}$:GUS* reporter gene construct in *bop1-1* and *bop1-4 bop2-11* plants. Previous experiments detected *AS2* transcripts in embryonic protoderm cells on the adaxial side of cotyledon primordia beginning at the heart stage (Iwakawa et al., 2002, 2007; Wu

et al., 2008). This expression pattern was observed until the torpedo stage in *AS2*$_{pro}$*:GUS* embryos. Bent-cotyledon stage embryos displayed strong GUS staining in the adaxial domain of the cotyledons (Figures 5A and 5D). As the embryos fully matured, *AS2*$_{pro}$*:GUS* activity appeared weaker in this domain, and after germination, GUS staining was no longer detected in the cotyledons.

Up until the torpedo stage, no difference in the *AS2* expression pattern between wild-type and *bop* embryos was detected. At the early bent-cotyledon stage, wild-type embryos displayed *AS2* promoter-driven GUS activity from the base to the tip of the cotyledons (Figures 5A and 5D). By contrast, in *bop1-1* and *bop1-4 bop2-11* embryos, *AS2*$_{pro}$*:GUS* activity was not detected in the proximal domain of the cotyledons near the SAM (Figures 5B, 5C, 5E, and 5F). Sagittal views confirm that GUS staining was absent from the proximal domain of *bop* embryonic cotyledons (Figures 5G to 5L), the region in which the *bop1-1* phenotype is detected after germination.

Next, we analyzed *AS2*$_{pro}$*:GUS* activity at the vegetative stage. Compared with wild-type seedlings (Figure 5M; see Supplemental Figures 6A and 6B online), GUS activity was reduced or absent in the leaf base of both *bop1-1* and *bop1-4 bop2-11* seedlings (Figures 5N and 5O; see Supplemental Figures 6C and 6D online). This region corresponds to the *BOP1* and *BOP2* expression domains (see Supplemental Figure 7 online), demonstrating that BOP1 and BOP2 are required during both embryonic and vegetative development to induce *AS2* expression in the proximal domain of cotyledons and rosette leaves.

Requirement of *AS2* for *bop* and *as* Leaf Phenotypes

Our data indicate that BOP1 and BOP2 are required to activate *AS2* expression in the proximal domain of cotyledons and leaves, the region in which the *bop* ectopic outgrowth phenotype is manifested. We tested whether the absence of proximal *AS2* activity is responsible for the *bop* phenotype by generating transgenic plants expressing *AS2* under the control of 6.0 kb of *BOP1* upstream sequence. When fused to a GUS reporter, this *BOP1* promoter sequence drives strong GUS activity at the base of the cotyledons and leaves, recapitulating the native *BOP1* expression domain (Figure 6J). We then determined whether driving *AS2* in the *BOP1* expression domain could rescue the *bop* proximal ectopic leaf outgrowth phenotypes (Figures 6A and 6C). Transformation of *BOP1*$_{pro}$*:AS2* into *bop1-4 bop2-11* and *bop1-1* plants led to the elevation of *AS2* expression levels (Figure 6I) and a dramatic reduction in the amount of ectopic outgrowth along the petioles (Figures 6B and 6D). Eleven percent of *bop1-1* lines ($n = 37$) and 5% of *bop1-4 bop2-11* lines ($n = 230$) showed phenotypic complementation (see Supplemental Table 1 online). Thus, the ectopic outgrowth in *bop* leaves is directly attributable to the loss of *AS2* expression in the proximal region of the primordia, indicating that BOP1 and BOP2 act through *AS2* to suppress meristematic activity and/or class I *KNOX* gene expression in this region.

Next, we assessed the ability of the *BOP1*$_{pro}$*:AS2* construct to rescue the *as1* and *as2* leaf phenotypes. *BOP1*$_{pro}$*:AS2 as1-1* plants (Figure 6H) were indistinguishable from *as1-1* plants (Figure 6G), indicating that *BOP1*$_{pro}$*:AS2* activity had no detectable

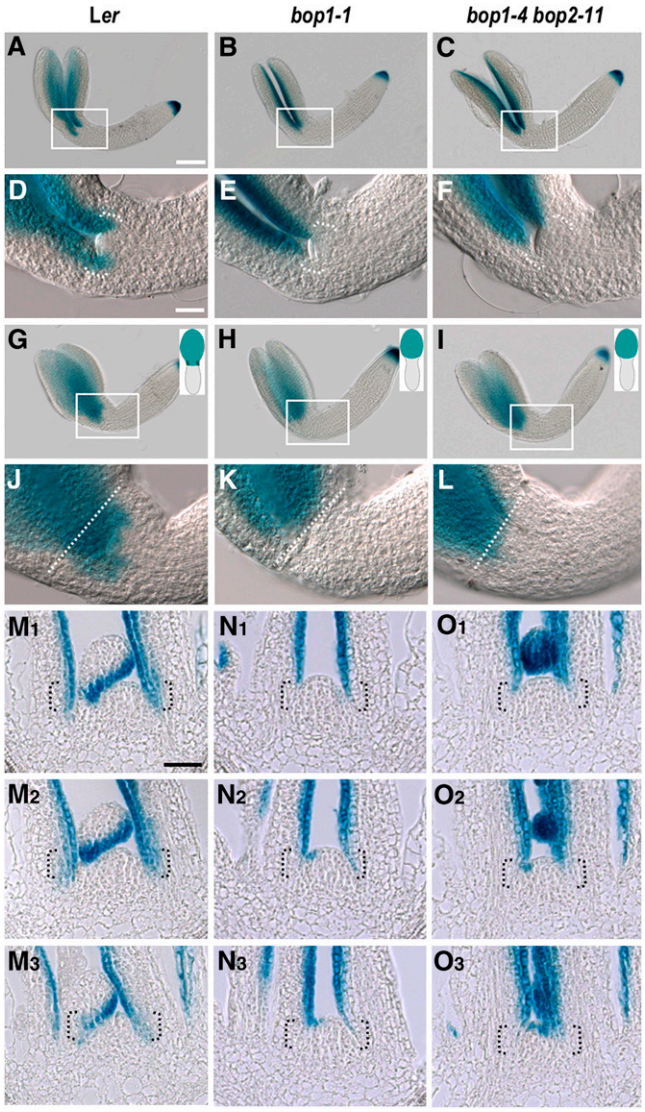

Figure 5. Polar Regulation of *AS2* Expression by BOP1 and BOP2.

(A) to **(F)** show a frontal view, and **(G)** to **(L)** show a sagittal view. **(D)** to **(F)** and **(J)** to **(L)** are magnified views of the regions boxed in **(A)** to **(C)** and **(G)** to **(I)**, respectively. A schematic of the sagittal view of the embryo on its side with one cotyledon atop the other is shown for **(G)** to **(L)**. In **(J)** to **(L)**, the dotted line marks the boundary between the cotyledon and cotyledonary petiole. In **(D)** to **(F)** and **(M)** to **(O)**, brackets denote the proximal organ region. Bars = 100 μm in **(A)** to **(C)**, **(G)** to **(I)**, and **(M)** to **(O)** and 25 μm in **(D)** to **(F)** and **(G)** to **(L)**.

(A), **(D)**, **(G)**, and **(J)** GUS activity in *AS2*$_{pro}$*:GUS Ler* bent-cotyledon stage embryos.

(B), **(E)**, **(H)**, and **(K)** GUS activity in *AS2*$_{pro}$*:GUS bop1-1* bent-cotyledon stage embryos.

(C), **(F)**, **(I)**, and **(L)** GUS activity in *AS2*$_{pro}$*:GUS bop1-4 bop2-11* bent-cotyledon stage embryos.

(M) Serial sections of a 10-d-old *AS2*$_{pro}$*:GUS Ler* shoot apex.

(N) Serial sections of a 10-d-old *AS2*$_{pro}$*:GUS bop1-1* shoot apex.

(O) Serial sections of a 10-d-old *AS2*$_{pro}$*:GUS bop1-4 bop2-11* shoot apex.

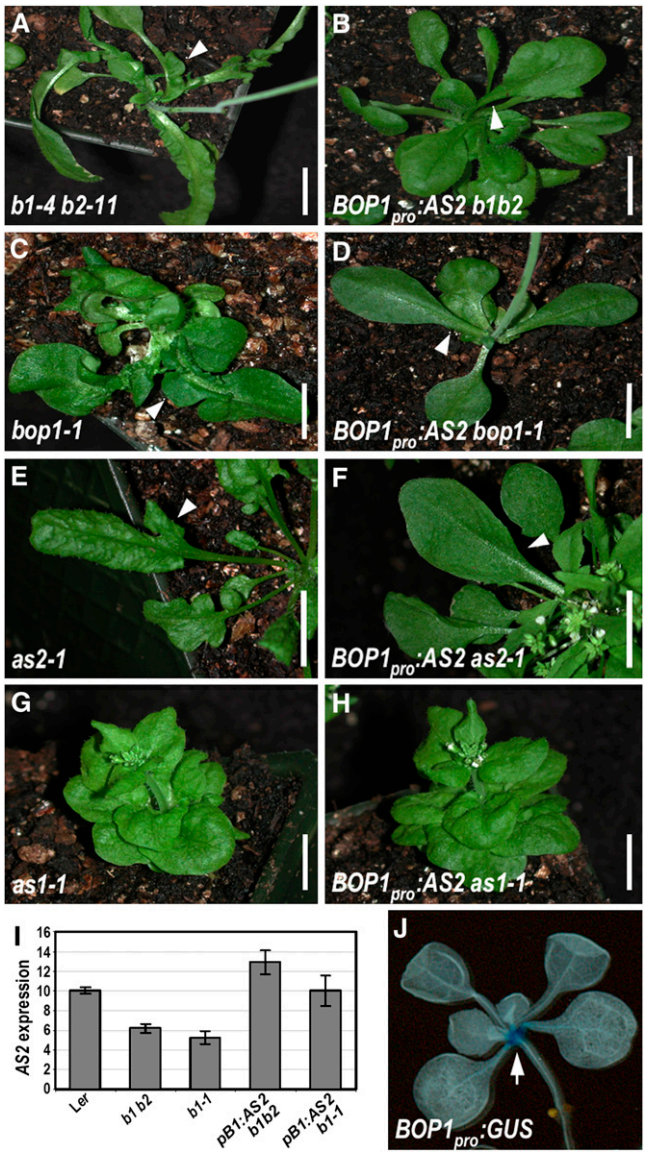

Figure 6. Rescue of the *bop* Phenotype by a $BOP1_{pro}$*:AS2* Transgene.

(A) *bop1-4 bop2-11* rosette.
(B) $BOP1_{pro}$*:AS2 bop1-4 bop2-11* rosette.
(C) *bop1-1* rosette.
(D) $BOP1_{pro}$*:AS2 bop1-1* rosette.
(E) *as2-1* rosette.
(F) $BOP1_{pro}$*:AS2 as2-1* rosette.
(G) *as1-1* rosette.
(H) $BOP1_{pro}$*:AS2 as1-1* rosette.
(I) *AS2* expression in wild-type L*er*, *bop1 bop2* (*b1 b2*), *bop1-1* (*b1-1*), and $BOP1_{pro}$*:AS2* plants. Mean transcript levels were determined by real-time quantitative PCR analyses and normalized to *EF1*α. Error bars represent SD.
(J) $BOP1_{pro}$*:GUS* activity in a Col seedling.
Arrowheads indicate ectopic organ outgrowths in **(A)** and **(C)**, rescued leaf morphology in **(B)**, **(D)**, and **(F)**, and lobed leaf morphology in **(E)**. The arrow in **(J)** indicates the leaf base around the SAM. Bars = 10 mm.

effect on the *as1* phenotype. By contrast, $BOP1_{pro}$*:AS2 as2-1* plants displayed rescue of the *as2-1* leaf phenotype (Figures 6E and 6F; see Supplemental Table 1 online). This result indicates that the expression of *AS2* exclusively in the BOP1 domain at the proximal end of developing leaf primordia is sufficient to confer wild-type leaf morphology.

Relationship between the BOP and STM Pathways

Mutations in *AS2* (and *AS1*) suppress the *stm* embryonic and vegetative SAM phenotypes, an effect that in the case of *AS1* is *BP* dependent (Byrne et al., 2000, 2002). Finding that *BOP1* and *BOP2* induce *AS2* expression near the boundary between the SAM and leaf primordia, we used genetic analysis to investigate whether *BOP1* and *BOP2* affect the *STM* pathway.

Plants homozygous for the strong *stm-11* allele lacked an embryonic SAM (Long et al., 1996; Carles et al., 2004) and formed cotyledons that were fused at their base (Figure 7C), unlike wild-type plants (Figure 7B), yet 20 d after germination, 10% of *stm-11* plants (n = 56 for experiment i and 166 for experiment ii) developed rosette leaves from either the shoot apex or the region between the fused cotyledonary petioles (Figure 7A). At germination, *bop1-4 bop2-11 stm-11* seedlings appeared identical to *stm-11* seedlings. However, 6 to 7 d later, some triple mutant seedlings began to develop leaves from the fused cotyledonary petiole region (Figure 7D), and by 13 d after germination, 100% of *bop1 bop2 stm* plants (n = 57 for i and 34 for ii) had formed a shoot meristem and produced true leaves from this region (Figure 7A). Compared with dome-shaped wild-type SAMs, which consisted of small, highly cytoplasmic cells organized into discrete cell layers, the flattened shoot apex region of *stm-11* seedlings contained large, vacuolated cells (see Supplemental Figure 8 online). Sections through the fused cotyledonary petiole region of *bop1 bop2 stm* seedlings revealed within the differentiated tissue the presence of domes of small, highly cytoplasmic cells resembling those of wild-type shoot meristems, albeit somewhat less organized (see Supplemental Figure 8 online). Thus, the absence of the BOP proteins in *stm-11* plants permits the formation of a functional shoot meristem at the base of the fused cotyledons.

In *as1 stm* plants, *BP* can replace *STM* to promote embryonic and vegetative SAM formation (Byrne et al., 2002). To determine if *BP* is likewise necessary for the meristematic activity observed in *bop1 bop2 stm* plants, we constructed *bop1-4 bop2-11 stm-11 bp-1* plants. We found that compared with 100% of *bop1-4 bop2-11 stm-11* seedlings, only 30 to 40% of *bop1-4 bop2-11 stm-11 bp-1* seedlings initiated a postembryonic shoot meristem (n = 37 for i and 57 for ii) (Figure 7A). These data indicate that, in the absence of *BOP* activity, *BP* can substitute for *STM* to establish a functional vegetative shoot meristem.

AS1 expression expands ectopically into the apical region of *stm* embryos, indicating that *AS1* is negatively regulated by *STM* (Byrne et al., 2000). Genetic models propose that *AS2* is also negatively regulated by STM (Byrne et al., 2002); however, this has not been demonstrated at the molecular level. To determine the relationship between *STM* and *AS2*, we examined $AS2_{pro}$*:GUS* activity during *stm-11* embryo development. Unlike *AS1*, *AS2* was not ectopically expressed in *stm-11* embryos until the

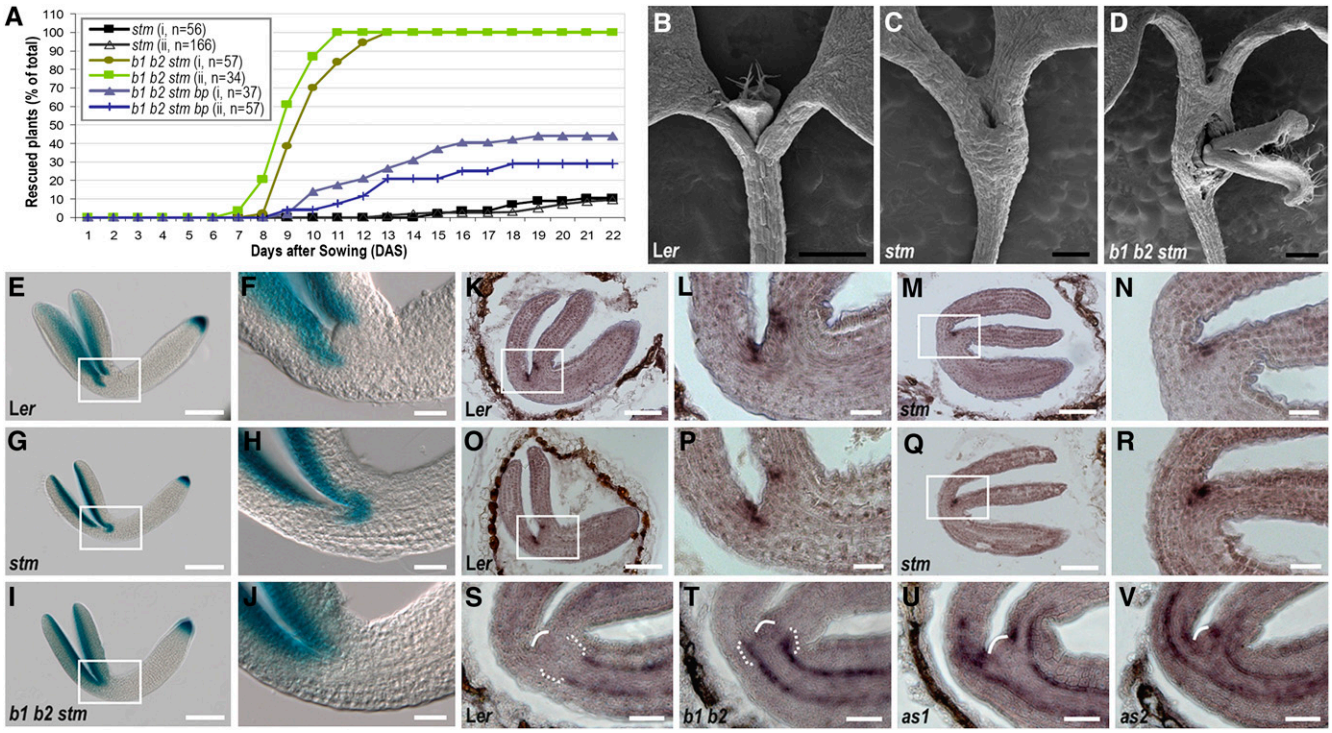

Figure 7. Genetic Interactions between *BOP* and the *STM-AS2* Pathway.

(A) Rescue of *stm-11* phenotypes by *bop1-4 bop2-11* and *bp-1*. Plants with organogenesis from the fused cotyledon region were counted as rescued. (i) and (ii) represent separate experiments.
(B) to **(D)** Scanning electron micrographs of 7-d-old L*er* **(B)**, *stm-11* **(C)**, and *bop1-4 bop2-11 stm-11* **(D)** plants.
(E) to **(J)** $AS2_{pro}$*:GUS* activity in bent-cotyledon stage embryos.
(E) and **(F)** L*er*.
(G) and **(H)** *stm-11*.
(I) and **(J)** *bop1-4 bop2-11 stm-11*.
(K) to **(N)** *BOP1* expression in bent-cotyledon stage embryos.
(K) and **(L)** L*er*.
(M) and **(N)** *stm-11*.
(O) to **(R)** *BOP2* expression in bent-cotyledon stage embryos.
(O) and **(P)** L*er*.
(Q) and **(R)** *stm-11*.
(S) to **(V)** *BP* expression in bent-cotyledon stage embryos.
(S) L*er*.
(T) *bop1-4 bop2-11*.
(U) *as1-1.*
(V) *as2-1*.
(F), **(H)**, **(J)**, **(L)**, **(N)**, **(P)**, and **(R)** are magnified views of the regions boxed in **(E)**, **(G)**, **(I)**, **(K)**, **(M)**, **(O)**, and **(Q)**, respectively. In **(S)** to **(V)**, white arches denote the SAM, and brackets indicate the cotyledonary petiole region. Bars = 0.5 mm in **(B)** to **(D)**, 100 μm in **(E)**, **(G)**, **(I)**, **(K)**, **(M)**, **(O)**, and **(Q)**, and 25 μm in **(F)**, **(H)**, **(J)**, **(L)**, **(N)**, **(P)**, and **(R)** to **(V)**.

torpedo stage. In bent-cotyledon stage wild-type embryos, *AS2* expression was restricted to the adaxial region of the cotyledons (Figures 7E and 7F). In *stm-11* embryos, *AS2* was ectopically expressed at the junction between the fused cotyledons, where the SAM would normally have formed (Figures 7G and 7H; see Supplemental Table 2 online). Because ectopic activation of *AS2* was observed only after the *stm* phenotype was manifested, this result indicates that *AS2* expression is not directly regulated by STM, but rather by another factor functional in the SAM.

Given that *AS2* is an immediate target of *BOP* regulation, we compared the *BOP* and *AS2* embryo expression patterns. In wild-type embryos, *BOP1* (Figures 7K and 7L) and *BOP2* (Figures 7O and 7P) were expressed in two foci in the proximal, adaxial region of the developing cotyledons. In *stm-11* embryos, *BOP* expression was detected at the junction between the fused cotyledons (Figures 7M, 7N, 7Q, and 7R), coincident with the domain of ectopic *AS2* expression. However, in *bop1-4 bop2-11 stm-11* embryos, $AS2_{pro}$*:GUS* was not ectopically activated in this central region (Figures 7I and 7J). These data indicate that

STM directly or indirectly represses *BOP1* and *BOP2* expression in the wild-type embryonic SAM and that misexpression of *BOP1/2* at the junction between the fused cotyledons in *stm* embryos is responsible for the ectopic activation of *AS2* in this domain.

Rescued *bop1 bop2 stm* seedlings formed ectopic shoot meristems from the fused cotyledonary petiole region (Figure 7D), whereas *as1 stm* and *as2 stm* seedlings formed meristems at their shoot apices like *as1* and *as2* single mutants (Byrne et al., 2000, 2002). We reasoned that because *BP* can substitute for *STM* in *as1 stm* and *as2 stm* seedlings and is also partially responsible for the rescued phenotypes of *bop1 bop2 stm* seedlings (Figure 7A), the difference in phenotypic rescue between *as1 stm*, *as2 stm*, and *bop1 bop2 stm* seedlings might be due to the differential misregulation of *BP* expression. Thus, we compared the *BP* expression patterns in *as1*, *as2*, and *bop1 bop2* embryos. In wild-type embryos, *BP* mRNA was detected in two stripes in the procambium layer of the hypocotyl (Figure 7S; see Supplemental Figure 9A online). In *as1-1* and *as2-1* embryos, ectopic *BP* expression was observed in the basal region of the cotyledons and flanking the SAM (Figures 7U and 7V). By contrast, ectopic *BP* expression was not observed flanking the shoot apex in *bop1-4 bop2-11* embryos (Figure 7T). However, *BP* expression was expanded into the presumptive junction between the hypocotyl and cotyledon base (Figure 7T; see Supplemental Figures 9B and 9C online), the area corresponding to the region of de novo shoot meristem generation in *stm-11 bop1-4 bop2-11* seedlings (Figure 7D). Region-specific misregulation of *BP* expression can therefore account for the differences between the *as1 stm*, *as2 stm*, and *bop1 bop2 stm* embryo phenotypes, although interestingly, BOP-dependent *BP* suppression appears to be regulated nonautonomously.

DISCUSSION

The BOP1 and BOP2 proteins contain a conserved BTB/POZ domain, which has been shown to mediate protein–protein interactions and to confer transcription activation capacity to the related NPR1 protein (Rochon et al., 2006). We find that BOP1 and BOP2, like NPR1, can function as transcriptional activators when recruited to target DNA. Because they lack known DNA binding sequences, it seems likely that BOP1 and BOP2 act as transcriptional coactivators in vivo when recruited to the promoter region of target genes through their interaction with DNA binding proteins. BOP1 and BOP2 can physically interact with one another in vitro and in vivo, and bop1-1 mutant protein can interact with both wild-type proteins. In addition, bop1-1 protein strongly reduces the transactivation capability of the BOP1 and BOP2 proteins. Based on these data, we propose that the dominant-negative phenotype of the *bop1-1* plants is caused by the interference of bop1-1 mutant protein with wild-type BOP2 protein activity, causing *bop1-1* plants to resemble *bop1 bop2* double mutant plants.

NPR1 acts as a coactivator to regulate *Arabidopsis* defense gene expression (Cao et al., 1994). This coactivator function of NPR1 is mediated by SA-dependent protein modification, whereas recruitment of the protein to target promoters is autonomous and SA independent. In contrast with NPR1, BOP1 and BOP2 display transactivation activity independent of SA or other stimuli. Interestingly, the BOP proteins lack all or part of two domains of NPR1, one located from amino acids 22 to 44 and the other located from amino acids 463 to 513 (see Supplemental Figure 10 online), that repress transactivation activity in the absence of SA (Rochon et al., 2006). BOP1 and BOP2 also lack two Cys residues (Cys-521 and Cys-529) that modulate transactivation in SA-stimulated cells (Rochon et al., 2006). These specific structural differences between the BOP proteins and NPR1 may largely account for the lack of responsiveness of the BOP proteins to SA.

Recently it has been reported that *S*-nitrosylation on residue Cys-156 of NPR1 induced its oligomerization upon SA induction to maintain protein homeostasis (Tada et al., 2008). The BOP proteins lack the Cys residue that corresponds to Cys-156 of NPR1, whereas four other Cys residues in the BTB/POZ domain important for oligomerization (Mou et al., 2003) appear to be conserved (see Supplemental Figure 10 online). Because the BOP proteins localize to both the nucleus and the cytosol without any stimulus, the absence of the Cys-156 residue can be considered one structural feature that releases their subcellular localization from SA regulation. Nuclear localization of BOP1 protein is necessary and sufficient for its biological function; thus, cytoplasmic retention of BOP1 protein might maintain protein homeostasis. However, it remains to be seen whether regulated nuclear transport exists for the BOP proteins and whether they respond to a developmental signal(s) as has been previously proposed (Hepworth et al., 2005).

BOP1 and BOP2 are positive regulators of *AS2* transcription. Among the known BOP1 and BOP2 target genes, only the expression of *AS2* was rapidly induced by $35S_{pro}$*:BOP1-GR*, indicating that it is an early target of the BOP pathway. Induction of *AS2* expression by BOP1 did not require protein synthesis, consistent with *AS2* being a direct target of BOP1. By contrast, *ASL4*/*LOB* showed delayed induction compared with that of *AS2*. Because AS2 positively regulates *ASL4*/*LOB* expression (Byrne et al., 2002), *ASL4*/*LOB* regulation by BOP protein could be mediated through AS2. The regulation of adaxial-abaxial polarity genes by *BOP1* and *BOP2* (Ha et al., 2007) may also be mediated partially or fully through AS2. *AS2* being a major target of BOP activity is also consistent with the observation that driving *AS2* transcription in the *BOP1* expression domain is sufficient to partially rescue the *bop* phenotype in some plants. However, the fact that the percentage of rescued plants is low indicates that additional target genes, as yet to be identified, also play biologically relevant roles in the BOP leaf morphogenesis regulatory pathway.

We find that BOP1 protein is specifically recruited to the *AS2* promoter where it can function as part of a transcriptional activator complex to induce *AS2* expression. The promoter elements with which BOP1 associates are positioned between 2.6 and 3.2 kb upstream of the *AS2* start site. This is considerably upstream of a binding site for KAN1, a negative regulator of *AS2*, which lies 1.4 kb upstream of the ATG (Wu et al., 2008). Because the BOP proteins lack a discernable DNA binding domain, no information is available about the specific *cis*-element(s) with which BOP1 may associate at the *AS2* promoter. However, the

genomic region responsible for the BOP1-mediated induction of *AS2* expression coincides with the region to which BOP1 protein binds in vivo. This region contains an A-box bZIP transcription factor binding site, the presence of which may indicate involvement of TGA transcription factors in BOP1 DNA binding, as has been proposed for NPR1 (Rochon et al., 2006). BOP proteins physically interact with the TGA transcription factor PERIANTHIA (PAN) in yeast (Hepworth et al., 2005), and the fact that *bop1 bop2* and *pan* plants have overlapping phenotypes indicates that they function in the same genetic pathway. However, neither BOP1 nor BOP2 modulate the transcriptional activity of PAN in transactivation assays nor is *AS2* transcription regulated by PAN (see Supplemental Figure 11 online). We therefore predict that the BOP proteins may regulate *AS2* expression in concert with multiple bZIP transcription factor family members.

The AS1-AS2 chromatin-remodeling complex plays a key role in class I *KNOX* gene repression in *Arabidopsis* lateral organs (Guo et al., 2008); conversely, *AS1* is negatively regulated by *STM* in the SAM to maintain these cells in a proliferative state (Byrne et al., 2000). However, the regulatory mechanism that excludes *AS2* from the SAM has not been understood. Our study shows during the early stages of *stm* embryogenesis, *AS2* expression is excluded from the presumptive shoot apex region and is ectopically expressed only at a late stage of embryo development when the *stm* phenotype is already evident. Thus, *AS2* is regulated by a factor functional in the SAM region, but not directly by *STM*. At the late embryonic stage, *AS2* expression adjacent to the shoot apex is dependent on BOP function in both wild-type and *stm* plants. This finding implicates *BOP* function in the suppression of meristematic activity during late embryogenesis through the induction of *AS2* in the adaxial, proximal region of the cotyledons.

Our results also uncover mutual negative regulation between the *BOP* genes and the class I *KNOX* genes. We find that *STM* directly or indirectly represses *BOP1* and *BOP2* expression in the SAM and that the ectopic activation of *AS2* across the shoot apex region of *stm* embryos is dependent on BOP activity. Furthermore, the *BOP* genes (as well as *AS1* and *AS2*) negatively regulate embryonic *BP* expression at the hypocotyl-cotyledon junction, such that in the absence of *BOP* activity, *BP* can substitute for *STM* to establish a functional vegetative shoot meristem following germination. Interestingly, we observed that in *as1*, *as2*, and *bop1 bop2* embryos, *BP* misexpression occurred at the hypocotyl-cotyledon junction in two stripes of cells in the procambium layer that do not normally express *AS1*, *AS2*, or the *BOP* genes. These data suggest that, in addition to their roles in lateral organ determinacy and patterning, these genes act non-cell-autonomously to repress *BP* transcription. It remains to be seen whether this non-cell-autonomous activity of BOP1 and BOP2 is mediated via their regulation of *AS2*.

The molecular mechanisms that establish pattern formation along the proximal-distal leaf axis are still poorly defined. Leaf differentiation occurs from the distal blade toward the proximal petiole, reflected by a cell cycle arrest front moving gradually from tip to base (Nath et al., 2003). Studies have shown that growing leaves display a gradient of cell division rates in which the highest rates occur in the proximal regions (Poethig and Sussex, 1985). Class I *KNOX* gene activity creates an environment that promotes and sustains cell proliferation, and their ectopic expression in developing leaves prolongs leaf cell division and confers indeterminate features such as lobing and ectopic meristem formation (Chuck et al., 1996).

The formation of ectopic outgrowths of blade tissue along the leaf petiole accompanied by ectopic *KNOX* gene expression in *bop1-1* and *bop1 bop2* mutants indicates that BOP1 and BOP2 are redundantly required for *KNOX* repression in the proximal region of developing leaves (Ha et al., 2003, 2007). Furthermore, *BOP1* and *BOP2* are expressed specifically in the proximal, adaxial region of the leaf beginning at the time of primordia initiation. The *BOP* expression domain overlaps with that of *AS2* (Iwakawa et al., 2007), and BOP activity is required to induce *AS2* transcription in the proximal, adaxial region of organ primordia. In addition, the *BOP* genes and *AS2* promote adaxial organ identity (Lin et al., 2003; Xu et al., 2003; Ha et al., 2007). *as2* and *bop* mutants have some overlapping phenotypes, although the *bop* phenotype is more severe than the *as2* phenotype in proximal tissues. However, *bop as2* plants display a synergistic phenotype (Ha et al., 2003, 2007), indicating that *AS2* and the *BOP* genes are part of overlapping genetic pathways rather than a single linear pathway. Therefore, the *BOP* genes likely regulate other factors in the proximal leaf domain in addition to *AS2*, potentially including other *ASL/LBD* genes. However, ectopic *BOP* activity does not suppress normal blade development. This suggests that the function of the *BOP* genes as suppressors of blade formation is executed within a certain developmental context in the proximal region of the leaf.

An additional target of *BOP* proximal-distal regulation is the C2H2 zinc-finger putative transcription factor gene *JAGGED* (*JAG*). Loss-of-function *jag* mutations result in incomplete

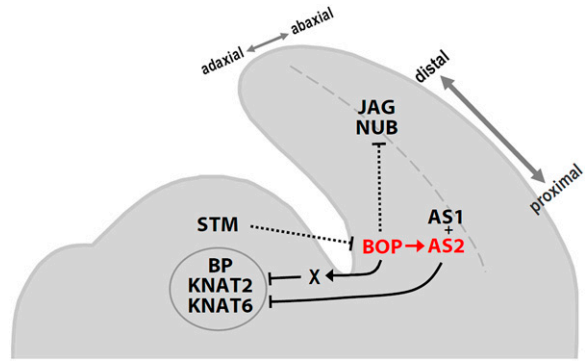

Figure 8. Model for *Arabidopsis* Vegetative Organ Initiation and Patterning.

The class I *KNOX* protein STM is restricted to the SAM and represses the expression of organ patterning genes, such as *BOP1* and *BOP2* (BOP). The *BOP* genes are transcribed at the adaxial base of vegetative primordia, where they directly activate *AS2* expression and directly or indirectly repress *JAG* and *NUB* expression in the proximal domain to pattern the proximal-distal axis. AS2 and AS1 form a protein complex that is active throughout the adaxial organ domain and directly represses *BP* and *KNAT2* transcription to restrict their activity to the SAM. The BOP proteins also repress *BP*, *KNAT2*, and *KNAT6* transcription in the proximal region of organ primordia, likely indirectly through an unknown factor (X).
[See online article for color version of this figure.]

formation of distal tissues in developing leaves and floral organs, which is associated with the premature cessation of cell division (Dinneny et al., 2004; Ohno et al., 2004). Ectopic *JAG* expression in *jag-5D* mutants causes the formation of ectopic blade tissue along the leaf petiole (Dinneny et al., 2004), similar to the loss-of-function *bop* phenotypes. The specific role of *JAG* in promoting leaf growth suggests that it acts downstream of leaf patterning genes; indeed, BOP1 and BOP2 repress the expression of *JAG* and its close relative *NUBBIN* (*NUB*; aka *JGL*) in the proximal leaf domain (Norberg et al., 2005).

Our data that BOP1 is required to specifically induce *AS2* expression in proximal cotyledon and rosette leaf cells begins to uncover a molecular mechanism for *Arabidopsis* proximal-distal polarity establishment (Figure 8). The *BOP* and *AS2* expression patterns at the base of the leaf primordia are mutually exclusive with the class I *KNOX* gene expression patterns in the SAM (Pautot et al., 2001; Belles-Boix et al., 2006), and the proximal *BOP* expression pattern is reciprocal to the distal *JAG* and *NUB* expression patterns (Dinneny et al., 2004; Ohno et al., 2004). During organ patterning, BOP1/2 operate in the proximal region of the primordia to induce the transcription of *AS2* and other target genes to suppress inappropriate class I *KNOX* gene activation. They also directly or indirectly repress *JAG* and *NUB* expression, restricting their activity to distal leaf cells. The sum of these activities promotes determinacy in proximal leaf cells, ensuring the proper specification of petiole tissue adjacent to the SAM.

METHODS

Plant Materials

Arabidopsis thaliana plants were grown as described (Ha et al., 2004). All plants, including *bop1-1* (Ha et al., 2003), *bop1-4 bop2-11* (Ha et al., 2004), *as1-1* (Byrne et al., 2000) *stm-11* (Long and Barton, 1998), and *bp-1* (Venglat et al., 2002), were in the L*er* ecotype, except for *pan-1* in the Wassilewskija background (Hepworth et al., 2005) and those plants carrying the *as2-1* allele (Semiarti et al., 2001), which were introgressed three times into Columbia (Col-0) prior to analysis. The $35S_{pro}$*:BOP1* line was previously described (Ha et al., 2007).

Construction of Transgenic Plants

The *BOP1-GR* fusion construct was created by cloning the *BOP1* full-length cDNA into the *Bam*HI and *Xho*I restriction sites of the GR vector (Huq et al., 2004). The $BOP1_{pro}$*:AS2* construct was generated by cloning 6.0 kb of *BOP1* upstream sequence into pCAMBIA1302 (CAMBIA) adjacent to a full-length *AS2* cDNA using the *Eco*RI, *Pst*I, and *Bst*EII restriction sites. To generate the *GUS* constructs, regions of the *AS2* upstream sequence or the 6.0-kb *BOP1* upstream sequence were amplified from Col genomic DNA and blunt end cloned into pENTR/D-TOPO (Invitrogen), then recombined into pBGWFS7,0 using Gateway LR recombination (Invitrogen). The full-length 4.8-kb promoter region of *AS2* was used to generate the $AS2_{pro}$*:GUS* reporter construct. For each construct, the binary vector in the *Agrobacterium tumefaciens* strain GV3101 was introduced into plants by the floral dip method (Clough and Bent, 1998). Primer sequences are listed in Supplemental Table 3 online.

Transactivation Assays

For the Gal4 DNA BD fusions, the *BOP1*, *BOP2*, or *bop1-1* coding sequences were cloned into the *Bam*HI and *Kpn*I restriction sites in frame to the BD in the pMN6 plasmid (Huq et al., 2003). Primer sequences are given in Supplemental Table 3 online. pMN6 alone was used as a negative control. A Renilla luciferase (LUC) gene under the control of a cauliflower mosaic virus 35S promoter was used as an internal control, and a firefly LUC gene under the control of four copies of the Gal4 upstream activating sequence fused to a minimal promoter served as a reporter (Huq et al., 2003). The LUC gene in the pGLL reporter plasmid (Huq et al., 2003) was driven by a chimeric promoter containing two copies of the lac operator and four copies of the Gal4 binding site fused upstream of a minimal 35S promoter fragment. Col whole seedlings or leaves were bombarded with the effector constructs along with the 4× USAGal4: firefly luciferase reporter and the cauliflower mosaic virus 35S:renilla luciferase internal standard vector. For the bop1-1 transactivation assays, the BD-bop1-1 construct was cobombarded with either the BD:BOP1 or the BD-BOP2 construct at two different ratios (2.5:1 and 1:1). Up to 5 μg of each effector and reporter plasmid, as well as 0.2 μg of internal control plasmid, were delivered to the tissues by particle bombardment. Tissue was extracted in LUC extraction buffer (Roche). Transcription activity was measured using the dual-Luciferase system (Promega) from three bombardments repeated three times.

Yeast Two-Hybrid Assays

The coding sequences of *BOP1*, *BOP2*, or *bop1-1* were blunt end cloned into the pENTR/D-TOPO vector (Invitrogen) and then fused into the pDEST 32 BD and pDEST 22 AD vectors (Invitrogen) using Gateway LR recombination (Invitrogen). Primer sequences are given in Supplemental Table 3 online. The bait and prey constructs were transformed into the yeast strain MaV203 (MATα). β-Gal activity in transformed yeast cells was measured using *o*-nitrophenyl-β-D-galactopyranoside as the substrate according to the manufacturer's protocol (Invitrogen).

Expression Analysis

GUS staining, tissue embedding, and sectioning were performed as described (Sieburth and Meyerowitz, 1997). Plant fixation and in situ hybridization were performed as described (Jackson, 1992). Probes were generated with the primers given in Supplemental Table 3 online, except for *BP*, which was directly linearized from a plasmid provided by Sarah Hake (University of California at Berkeley). For the chemical induction treatments, whole seedlings were transferred into and immersed in Murashige and Skoog media containing 10 μM Dex and/or 50 μM CHX.

Total RNA extraction and RT-PCR was performed as described (Ha et al., 2007). Quantitative real-time PCR was performed using the SYBR Green PCR master mix (Applied Biosystems with the primers shown in Supplemental Table 3 online). PCR reactions were run and analyzed using a MyiQTM Single-Color real-time PCR detection system (Bio-Rad). Quantification of all real-time PCR experiments was performed using three biological replicates.

Bimolecular Fluorescence Complementation Assays

The coding sequences of *BOP1*, *BOP2*, or *bop1-1* were blunt end cloned into the pENTR/D-TOPO vector (Invitrogen) and fused to the dissected YFP at the N or C terminus in pE-SPYNE-GW (N-terminal) or pE-SPYCE-GW (C-terminal) (Weltmeier et al., 2006) using Gateway LR recombination (Invitrogen). Five micrograms of each YFP fusion construct plasmid and 200 ng of a pRecA-red fluorescent protein construct (Thompson et al., 2009) were used. For transient expression in onion cells, particle bombardment was performed using a Biollistic PDS-1000/He unit (Bio-Rad). For fluorescence visualization, epidermal peels were examined 24 h after bombardment using a Zeiss Axiophot microscope.

ChIP

ChIP was performed as described (Lawrence et al., 2004) using an anti-GR antibody (Santa Cruz Biotechnology) on seedlings mock or Dex treated for 4 h. Quantification of immunoprecipitated DNA was performed by real-time PCR. Comparison of the abundance of promoter fragments in +Dex versus –Dex treated *35S$_{pro}$:BOP1-GR bop1-1* plants was performed by first normalizing each amplification value to the unrelated *TUB4* sequence and then dividing by the value for input samples to obtain input-normalized values. The relative abundance of fragments in +Dex versus –Dex treated samples was calculated by determining the ratio of these input-normalized values. Primer sequences are listed in Supplemental Table 3 online.

Accession Numbers

Sequence data from this article can be found in the Arabidopsis Genome Initiative or GenBank/EMBL databases under the following accession numbers: BOP1 (AT3G57130), BOP2 (AT2G41370), AS2 (AT1G65620), ASL4/LOB (AT5G63090), LBD36 (AT5G66870), STM (AT1G62360), BP (AT4G08150), KNAT2 (AT1G70510), KNAT6 (AT1G23380), PHB (AT2G34710), FIL (AT2G45190), JAG (AT1G68480), NUB (AT1G13400), and PAN (AT1G68640).

Supplemental Data

The following materials are available in the online version of this article.

Supplemental Figure 1. Subcellular Localization of BOP1 Protein.

Supplemental Figure 2. Dex-Dependent Enrichment of BOP1-GR in the Nuclear Fraction.

Supplemental Figure 3. Phenotypes of L*er* and *bop1-1* Plants after Dex Treatment.

Supplemental Figure 4. Phenotypes of *35S$_{pro}$:BOP1-GR bop1-4 bop2-11* Plants.

Supplemental Figure 5. Direct Regulation of *AS2* Expression by BOP1.

Supplemental Figure 6. Polar Regulation of *AS2* Expression by BOP in Seedlings.

Supplemental Figure 7. Comparison of *AS2*, *BOP1*, and *BOP2* Expression Patterns.

Supplemental Figure 8. Ectopic Shoot Meristem Formation in Rescued *stm-11* Plants.

Supplemental Figure 9. Regulation of Embryonic *BP* Expression by *BOP1* and *BOP2*.

Supplemental Figure 10. Multiple Sequence Alignment of the BOP1, BOP2, and NPR1 Proteins.

Supplemental Figure 11. Analysis of the Relationship between BOP, AS2, and PAN.

Supplemental Table 1. Rescue of Leaf Phenotypes by the *BOP1$_{pro}$:AS2* Construct.

Supplemental Table 2. *AS2$_{pro}$:GUS* Expression in Wild-Type, *stm*, and *stm bop1 bop2* Embryos.

Supplemental Table 3. Oligonucleotides Used in This Study.

Supplemental Methods. Protein Detection, Construction of Transgenic Plants, Expression Analysis, and Histological Analysis.

Supplemental References.

ACKNOWLEDGMENTS

We acknowledge the ABRC for supplying seeds and thank Sarah Hake, Hirokazu Tsukaya, and members of the lab for helpful comments. This work was supported by a USDA Current Research Information System grant to J.C.F.

Received August 17, 2009; revised December 14, 2009; accepted January 12, 2010; published January 29, 2010.

REFERENCES

Abel, S., Nguyen, M.D., and Theologis, A. (1995). The PS-IAA4/5-like family of early auxin-inducible mRNAs in *Arabidopsis thaliana.* J. Mol. Biol. **251:** 533–549.

Belles-Boix, E., Hamant, O., Witiak, S.M., Morin, H., Traas, J., and Pautot, V. (2006). *KNAT6*: An *Arabidopsis* homeobox gene involved in meristem activity and organ separation. Plant Cell **18:** 1900–1907.

Byrne, M.E., Barley, R., Curtis, M., Arroyo, J.M., Dunham, M., Hudson, A., and Martienssen, R.A. (2000). *Asymmetric leaves1* mediates leaf patterning and stem cell function in *Arabidopsis.* Nature **408:** 967–971.

Byrne, M.E., Simorowski, J., and Martienssen, R.A. (2002). *ASYMMETRIC LEAVES1* reveals *knox* gene redundancy in *Arabidopsis.* Development **129:** 1957–1965.

Cao, H., Bowling, S.A., Gordon, S., and Dong, X. (1994). Characterization of an *Arabidopsis* mutant that is nonresponsive to inducers of systemic acquired resistance. Plant Cell **6:** 1583–1592.

Cao, H., Glazebrook, J., Clarke, J.D., Volko, S., and Dong, X. (1997). The Arabidopsis NPR1 gene that controls systemic acquired resistance encodes a novel protein containing ankyrin repeats. Cell **88:** 57–63.

Carles, C.C., Lertpiriyapong, K., Reville, K., and Fletcher, J.C. (2004). The *ULTRAPETALA1* gene functions early in Arabidopsis development to restrict shoot apical meristem activity, and acts through *WUSCHEL* to regulate floral meristem determinacy. Genetics **167:** 1893–1903.

Chuck, G., Lincoln, C., and Hake, S. (1996). KNAT1 induces lobed leaves with ectopic meristems when overexpressed in *Arabidopsis*. Plant Cell **8:** 1277–1289.

Clough, S.J., and Bent, A.F. (1998). Floral dip: A simplified method for Agrobacterium-mediated transformation of *Arabidopsis thaliana*. Plant J. **16:** 735–743.

Despres, C., Chubak, C., Rochon, A., Clark, R., Bethune, T., Desveaux, D., and Fobert, P.R. (2003). The *Arabidopsis* NPR1 disease resistance protein is a novel cofactor that confers redox regulation of DNA binding activity to the basic domain/leucine zipper transcription factor TGA1. Plant Cell **15:** 2181–2191.

Despres, C., DeLong, C., Glaze, S., Liu, E., and Fobert, P.R. (2000). The *Arabidopsis* NPR1/NIM1 protein enhances the DNA binding activity of a subgroup of the TGA family of bZIP transcription factors. Plant Cell **12:** 279–290.

Dinneny, J.R., Yadegari, R., Fischer, R.L., Yanofsky, M.F., and Weigel, D. (2004). The role of *JAGGED* in shaping lateral organs. Development **131:** 1101–1110.

Dockx, J., Quaedvlieg, N., Keultjes, G., Kock, P., Weisbeek, P., and Smeekens, S. (1995). The homeobox gene *ATK1* of *Arabidopsis thaliana* is expressed in the shoot apex of the seedling and in flowers and inflorescence stems of mature plants. Plant Mol. Biol. **28:** 723–737.

Guo, M., Thomas, J., Collins, G., and Timmermans, M.C. (2008). Direct repression of *KNOX* loci by the ASYMMETRIC LEAVES1 complex of *Arabidopsis.* Plant Cell **20:** 48–58.

Ha, C.M., Jun, J.H., Nam, H.G., and Fletcher, J.C. (2004). *BLADE-ON-PETIOLE1* encodes a BTB/POZ domain protein required for leaf morphogenesis in *Arabidopsis thaliana*. Plant Cell Physiol. **45:** 1361–1370.

Ha, C.M., Jun, J.H., Nam, H.G., and Fletcher, J.C. (2007). *BLADE-ON-PETIOLE1* and *2* control *Arabidopsis* lateral organ fate through regulation of LOB domain and adaxial-abaxial polarity genes. Plant Cell **19:** 1809–1825.

Ha, C.M., Kim, G.-T., Kim, B.C., Jun, J.H., Soh, M.S., Ueno, Y., Machida, Y., Tsukaya, H., and Nam, H.G. (2003). The *BLADE-ON-PETIOLE1* gene controls leaf pattern formation through the modulation of meristematic activity in *Arabidopsis*. Development **130:** 161–172.

Hepworth, S.R., Zhang, Y., McKim, S., Li, X., and Haughn, G. (2005). BLADE-ON-PETIOLE-dependent signaling controls leaf and floral patterning in *Arabidopsis*. Plant Cell **17:** 1434–1448.

Huq, E., Al-Sady, B., Hudson, M., Kim, C., Apel, K., and Quail, P.H. (2004). Phytochrome-interacting factor 1 is a critical bHLH regulator of chlorophyll biosynthesis. Science **305:** 1937–1941.

Huq, E., Al-Sady, B., and Quail, P.H. (2003). Nuclear translocation of the photoreceptor phytochrome B is necessary for its biological function in seedling photomorphogenesis. Plant J. **35:** 660–664.

Iwakawa, H., Iwasaki, M., Kojima, S., Ueno, Y., Soma, T., Tanaka, H., Semiarti, E., Machida, Y., and Machida, C. (2007). Expression of the ASYMMETRIC LEAVES2 gene in the adaxial domain of Arabidopsis leaves represses cell proliferation in this domain and is critical for the development of properly expanded leaves. Plant J. **51:** 173–184.

Iwakawa, H., Ueno, Y., Semiarti, E., Onouchi, H., Kojima, S., Tsukaya, H., Hasebe, M., Soma, T., Ikezaki, M., Machida, C., and Machida, Y. (2002). The ASYMMETRIC LEAVES2 gene of *Arabidopsis thaliana*, required for formation of a symmetric flat leaf lamina, encodes a member of a novel family of proteins characterized by cysteine repeats and a leucine zipper. Plant Cell Physiol. **43:** 467–478.

Jackson, D. (1992). In situ hybridization in plants. In Molecular Plant Pathology: A Practical Approach, D.J. Bowles, S.J. Gurr, and R. McPherson, eds (Oxford, UK: Oxford University Press), pp. 163–174.

Jackson, D., Veit, B., and Hake, S. (1994). Expression of maize KNOTTED1 related homeobox genes in the shoot apical meristem predicts patterns of morphogenesis in the vegetative shoot. Development **120:** 405–413.

Lawrence, R.J., Earley, K., Pontes, O., Silva, M., Chen, Z.J., Neves, N., Viegas, W., and Pikaard, C.S. (2004). A concerted DNA methylation/histone methylation switch regulates rRNA gene dosage control and nucleolar dominance. Mol. Cell **13:** 599–609.

Li, H., Xu, L., Wang, H., Yuan, Z., Cao, X., Yang, Z., Zhang, D., and Huang, H. (2005). The putative RNA-dependent RNA polymerase *RDR6* acts synergistically with *ASYMMETRIC LEAVES1* and *2* to repress *BREVIPEDICELLUS* and microRNA165/166 in *Arabidopsis* leaf development. Plant Cell **17:** 2157–2171.

Lin, W., Shuai, B., and Springer, P.S. (2003). The *Arabidopsis* LATERAL ORGAN BOUNDARIES-domain gene ASYMMETRIC LEAVES2 functions in the repression of KNOX gene expression and adaxial-abaxial patterning. Plant Cell **15:** 2241–2252.

Lincoln, C., Long, J., Yamaguchi, J., Serikawa, K., and Hake, S. (1994). A knotted1-like homeobox gene in *Arabidopsis* is expressed in the vegetative meristem and dramatically alters leaf morphology when overexpressed in transgenic plants. Plant Cell **6:** 1859–1876.

Long, J.A., and Barton, M.K. (1998). The development of apical embryonic pattern in Arabidopsis. Development **125:** 3027–3035.

Long, J.A., Moan, E.I., Medford, J.I., and Barton, M.K. (1996). A member of the KNOTTED class of homeodomain proteins encoded by the STM gene of Arabidopsis. Nature **379:** 66–69.

Matsumura, Y., Iwakawa, H., Machida, Y., and Machida, C. (2009). Characterization of genes in the *ASYMMETRIC LEAVES2*/*LATERAL ORGAN BOUNDARIES* (*AS2*/*LOB*) family in *Arabidopsis thaliana* and functional and molecular comparisons between AS2 and other family members. Plant J. **58:** 525–537.

Mou, Z., Fan, W., and Dong, X. (2003). Inducers of plant systemic acquired resistance regulate NPR1 function through redox changes. Cell **113:** 935–944.

Nath, U., Crawford, B.C.W., Carpenter, R., and Coen, E. (2003). Genetic control of surface curvature. Science **299:** 1401–1407.

Norberg, M., Holmlund, M., and Nilsson, O. (2005). The BLADE ON PETIOLE genes act redundantly to control the growth and development of lateral organs. Development **132:** 2203–2213.

Ohno, C., Reddy, G.V., Heisler, M.G.B., and Meyerowitz, E.M. (2004). The *Arabidopsis JAGGED* gene encodes a zinc finger protein that promotes leaf tissue development. Development **131:** 1111–1122.

Ori, N., Eshed, Y., Chuck, G., Bowman, J.L., and Hake, S. (2000). Mechanisms that control knox gene expression in the Arabidopsis shoot. Development **127:** 5523–5532.

Pautot, V., Dockx, J., Hamant, O., Kronenberger, J., Grandjean, O., Jublot, D., and Traas, J. (2001). KNAT2: Evidence for a link between Knotted-like genes and carpel development. Plant Cell **13:** 1719–1734.

Phelps-Durr, T.L., Thomas, J., Vahab, P., and Timmermans, M.C. (2005). Maize rough sheath2 and its *Arabidopsis* ortholog ASYMMETRIC LEAVES1 interact with HIRA, a predicted histone chaperone, to maintain knox gene silencing and determinacy during organogenesis. Plant Cell **17:** 2886–2898.

Poethig, R.S., and Sussex, I.M. (1985). The cellular parameters of leaf development in tobacco: A clonal analysis. Planta **165:** 170–184.

Rochon, A., Boyle, P., Wignes, T., Fobert, P.R., and Despres, C. (2006). The coactivator function of *Arabidopsis* NPR1 requires the core of its BTB/POZ domain and the oxidation of C-terminal residues. Plant Cell **18:** 3670–3685.

Semiarti, E., Ueno, Y., Tsukaya, H., Iwakawa, H., Machida, C., and Machida, Y. (2001). The ASYMMETRIC LEAVES2 gene of *Arabidopsis thaliana* regulates formation of a symmetric lamina, establishment of venation and repression of meristem-related homeobox genes in leaves. Development **128:** 1771–1783.

Shuai, B., Reynaga-Pena, C.G., and Springer, P.S. (2002). The LATERAL ORGAN BOUNDARIES gene defines a novel, plant-specific gene family. Plant Physiol. **129:** 747–761.

Sieburth, L.E., and Meyerowitz, E.M. (1997). Molecular dissection of the AGAMOUS control region shows that cis elements for spatial regulation are located intragenically. Plant Cell **9:** 355–365.

Tada, Y., Spoel, S.H., Pajerowska-Mukhtar, K., Mou, Z., Song, J., Wang, C., Zuo, J., and Dong, X. (2008). Plant immunity requires conformational changes of NPR1 via S-nitrosylation and thioredoxins. Science **321:** 952–956.

Thompson, B.E., Bartling, L., Whipple, C., Hall, D.H., Sakai, H., Schmidt, R., and Hake, S. (2009). Bearded-ear encodes a MADS box transcription factor critical for maize floral development. Plant Cell **21:** 2578–2590.

Ueno, Y., Ishikawa, T., Watanabe, K., Terakura, S., Iwakawa, H., Okada, K., Machida, C., and Machida, Y. (2007). Histone deacetylases and ASYMMETRIC LEAVES2 are involved in the establishment of polarity in *Arabidopsis* leaves. Plant Cell **19:** 445–457.

Venglat, S.P., Dumonceaux, T., Rozwadowski, K., Parnell, L., Babic, V., Keller, W., Martienssen, R., Selvaraj, G., and Datla, R. (2002). The homeobox gene BREVIPEDICELLUS is a key regulator of inflorescence architecture in Arabidopsis. Proc. Natl. Acad. Sci. USA **99:** 4730–4735.

Weltmeier, F., Ehlert, A., Mayer, C.S., Dietrich, K., Wang, X.,

Schütze, K., Alonso, R., Harter, K., Vicente-Carbajosa, J., Dröge-Laser, W. (2006). Combinatorial control of Arabidopsis proline dehydrogenase transcription by specific heterodimerisation of bZIP transcription factors. EMBO J. **25:** 3133–3343.

Wu, G., Lin, W., Huang, T., Poethig, R.S., Springer, P., and Kerstetter, R. (2008). KANADI1 regulates adaxial-abaxial polarity in *Arabidopsis* by directly repressing the transcription of *ASYMMETRIC LEAVES2.* Proc. Natl. Acad. Sci. USA **105:** 16392–16397.

Xu, L., Xu, Y., Dong, A., Sun, Y., Pi, L., Xu, Y., and Huang, H. (2003). Novel as1 and as2 defects in leaf adaxial-abaxial polarity reveal the requirement for ASYMMETRIC LEAVES1 and 2 and ERECTA functions in specifying adaxial identity. Development **130:** 4097–4107.

Zhang, Y., Fan, W., Kinkema, M., Li, X., and Dong, X. (1999). Interaction of NPR1 with basic leucine zipper protein transcription factors that bind sequences required for salicylic acid induction of the PR-1 gene. Proc. Natl. Acad. Sci. USA **96:** 6523–6528.